



TECHNICAL UNIVERSITY OF CLUJ-NAPOCA

ACTA TECHNICA NAPOCENSIS

Series: Applied Mathematics, Mechanics, and Engineering  
Vol. 65, Issue II, June, 2022

## THE 3D PRINTED ASTRONAUTICAL PROBE SIMULATION ANALYZING THE FREE-FALL

Sven MARICIC, Iva MRSA, Răzvan PĂCURAR, Zoran MRSA

**Abstract:** This paper presents the concept and study of a 3D printed prototype of the atmospheric probe. An instrument for weather and atmospheric measuring can be used for a search with specific design features. Due to solid technological growth, environmentally friendly materials can now be used in 3D printing techniques while retaining the requisite model characteristics. The proposed model will theoretically analyze the environmental consequences of pandemics like COVID-19. The stages of a model probe with structural cross-sectional details are presented. In calculations and Ansys fluent simulations, we tested the free fall study. Computer CAD model simulation is measured with the average free-fall time to arrive on Earth from a 21 km height in the atmosphere. The resulting speed field is simulated with the chosen drop speed. We determined the drag force by flow simulation for a set of 5 different heights (0, 500, 11000, 19000 and 19500 m) with appropriate air density, pressures, and velocity. The free fall-speed curves versus height are given for three sample masses: 0.2, 0.4, and 0.5 kg. Finally, the average time of free fall for samples of various weights can be determined and the curve interpolated.

**Key words:** Additive technologies, astronautical probe, CAD/CAM, Ansys Fluent simulation, COVID19 spreading control

### 1. INTRODUCTION

With the aim of natural resource preservation, the trend is to use eco-friendly fabrics. The new European plan for plastics is based on the Circular Economy concept – an increase in recycling quality, more recycling schemes, and higher plastic waste recycling rates would raise the demand for recycled plastics [1]. According to the same source it has been estimated that just five percent of the value of the materials used in plastic packaging is kept in the economy; the rest of the value is lost after a very brief first usage. The annual bill totals something in the range of €70 billion to €105 billion.

#### 1.1 Polymers in additive manufacturing

Using Fused filament fabrication (FFF) to fabricate 3D printed composites with much higher mechanical performance has become a cutting-edge and interdisciplinary research topic in the last decade [2]. Combining several environmental friendly materials in this process

is a relatively new approach, and there is a lack of detailed experimental data on the mechanical performance of structures manufactured by this process conditions, underscoring the need for further research to improve understanding of the mechanical behaviour of 3D printed composites [3]. Several researchers investigated the mechanical performance, dimensional accuracy, and surface roughness [4, 5] of graphene nanoplatelets (GNPs) reinforced composites that were 3D printed using bioplastic Poly Lactic Acid Polylactide (PLA) or composite parts with short carbon fiber (SCF) as the base material and the additive manufacturing (AM) as the manufacturing process. This process significantly contributed to the recent research and development of vast number of materials including also biomaterials for prototyping, but it faces limited materials and regulatory issues as well as some environmental questions [6]. 3D printing needs more development to compete with traditional methods in the mass production of ordinary goods because of its higher cost and generally lower speed, but its development in

recent years is significant [7-10]. For this type of production, at the moment, there is a space for improvement when the aspects of waste materials and environmental impact(s) are being taken into account. Raw material (powder with nickel, for example), process (consumption of energy) and product (post-treatment, rejection) have an impact on the environment [11]. Most desktop 3D printers currently utilise either acrylonitrile butadiene styrene (ABS) or polylactic acid (PLA) as a thermoplastic feedstock [12]. Primary differences between ABS and PLA based printers are feedstock origin and nozzle and baseplate temperatures during operation. Our data indicate that the 3D printer type can impact the magnitude of the particle emission. The general impression is that print with ABS results in more significant particle emission than print with PLA regarding the emission of ultrafine particles.

## 1.2 The environmental impact of 3D printing

Given the intense focus on improving AM technologies in the industrial and scientific communities, it is likely that these obstacles can be overcome in the next decades [13]. 3D printing novel framework for processes sustainability assessment and improvement by integrating the product Computer-Aided Design (CAD) and Life Cycle Assessment (LCA) was proposed [14]. Their literature survey indicates that due to the variety of processing procedures and materials used, positive and negative opinions exist for the environmental impact of 3D printing, and it is not easy to draw an exact conclusion. The most reasonable conclusion is that the environmental impact of 3D printing is case-by-case depending on the specific situation. Comprehensive assessment of 3DP from a global sustainability perspective contains a qualitative evaluation of 3DP-induced sustainability implications and quantifies changes in life cycle costs, energy, and CO<sub>2</sub> emissions globally by 2025 [15]. Environmental impact of manufacturing polymer products can be reduced using distributed manufacturing with existing low-cost open-source 3D printers when using PLA. This approach indicates that distributed manufacturing is technically viable

and environmentally beneficial because of reduced energy consumption and greenhouse gas emissions. Based on that, this paper presents a possible way of primary materials substitution with renewable or regenerative alternatives for 3D print. In the same time taking into account restructuring production and consumption toward environmentally sensitive ones. It has been estimated that eco-design, waste prevention, and reuse can bring net savings for EU businesses of up to EUR 600 billion, while at the same time reduce greenhouse gas emissions [16].

## 2. MATERIALS AND METHODS

A combined approach have been used, 3D printing simulation for model manufacturing simulation and Fluent simulating software for shape analysis. The probe's purpose is to measure important environmental parameters like temperature, pressure and oxygen level to name a few. Using environmental-friendly materials, for example, PLA, could significantly reduce production carbon footprint without compromising favourable aeronautical characteristics. In this research, a focus was put on creating a realistic 3D model computer simulation and analysis.

### 2.1 Ansys Fluent flow simulation

The free fall of the probe was simulated using Ansys Fluent flow software [17]. This software uses the discretization of a domain in a finite number of finite volumes. The 3D fluid domain is, due to rotational symmetry, represented by a vertical halfplane through the probe axis, with the probe part excluded. The equivalent transformed the flow of moving air around the fixed probe was simulated. The boundary conditions were defined as follows: inflow boundary with given velocity (varied from 5 to 50 ms<sup>-1</sup>), outflow boundary as given pressure boundary, probe boundary as stationary wall, symmetry boundary as axis, and the outer boundary as no stress boundary. The initial condition is the start of probe free fall from the 20 km height. The fluid flow equations consist of continuity (1) and momentum equations (2) (mathematical representations of laws of mass

preservation and the second Newton law of motion in the differential form). The turbulence  $k$ - $\varepsilon$  model was used for high Reynolds number flows, where turbulence kinetic viscosity is defined in terms of turbulence kinetic energy  $k$  and its rate of dissipation  $\varepsilon$  (3). Transport equations for  $k$  and  $\varepsilon$  are not shown here. The Navier Stokes equations (continuity and momentum equations) describe the fluid dynamics. The local continuity equation is given by:

$$\sum_{j=1}^2 \frac{\partial u_j}{\partial x_j} = 0 \quad (1)$$

where  $x_j, j = 1, 2$  are Cartesian coordinates and  $u_j, j = 1, 2$  are the corresponding fluid velocity components.

Two horizontal momentum equations for the  $x_j, j = 1, 2$  component is:

$$\frac{\partial u_i}{\partial t} + \sum_{j=1}^2 \frac{\partial (u_i u_j)}{\partial x_j} = \frac{-1}{\rho} \frac{\partial p}{\partial x_i} + \sum_{j=1}^2 \frac{\partial}{\partial x_j} \left[ \nu_t \left( \frac{\partial u_i}{\partial x_j} + \frac{\partial u_j}{\partial x_i} \right) - \frac{2}{3} \delta_{ij} k \right], i = 1, 2 \quad (2)$$

In the  $k - \varepsilon$  model the eddy viscosity is derived from turbulence parameters  $k$  and  $\varepsilon$  as follows:

$$\nu_t = C_\mu \frac{k^2}{\varepsilon} \quad (3)$$

The equations with described boundary conditions are solved approximately with a Fluent solver using the finite volume method. First, the solution is approximated by piecewise polynomial representation. Then the residuals are multiplied by test functions and partially integrated over each limited volume leading to a local “stiffness” matrix with unknown vertex values of the solution. These “stiffness” matrices are then added for all finite volumes giving global matrix form. Considering boundary conditions, the global matrix is inverted giving solutions in volume vortices.

### 3. 3D METEOROLOGICAL PLA PROBE

In probing design, a Fused filament fabrication (FFF) and environmentally friendly Polylactic acid or polylactide (PLA) material were used to obtain physical model representation.

### 3.1 Probe design and construction phase

In the first phase, we generated a CAD model by Autodesk Fusion 360. This software was used due to its flexibility and enhanced online collaboration tools. Fusion 360 offers 3D design, assembly, and finite element method (FEM) analysis. In the first phase, a conceptual method was developed. The conceptual sketch of the model is based on the spatial requirements of the measuring instrumentation. The next phase involves Computer Aided Design (CAD) and Computer Aided Manufacturing (CAM) with chosen parameters. After CAD phase simulations of the probe free fall from the area so-called Armstrong's belt at an average height above 20,000 m were performed. Figure 1 presents a section of the probe model with several components added.

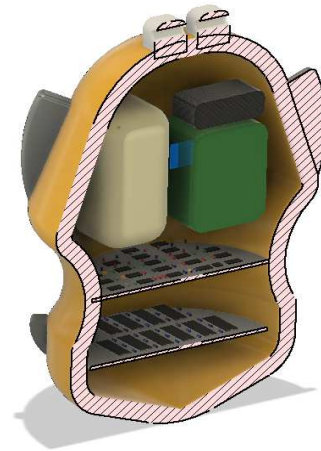


**Fig. 1.** Cross-section of probe model, interior section view with several added components

### 3.2 Material used in probe design and fabrication

Technical and mechanical properties (density, elastic modulus, tensile strength, coefficient of thermal expansion, flammability, melting point, specific heat capacity, thermal conductivity, dielectric constant, electrical resistivity, transparency) of the following materials have been compared: TIPPLEN K395, PP HOMO, HDPE, LDPE. For proposed materials: ABS, TPU, PLA, HIPS, PETG, NYLON, carbon fibre-filled, ASA, polycarbonate, polypropylene, metal filled, PVA, that had been evaluated, the value of the goal function was

calculated, defined as the weighted average of different properties: 30 % Ultimate strength, 20 % Durability, 30 % Density, 5 % Price, 5 % printability, 10 % recyclability [18]. We found the second-best (second biggest) goal function for PETG that possesses favourable characteristics for our purpose.

FFF processing of PETG requires high printing temperatures above 230 °C despite a low glass temperature of 77 °C [19]. The reason is the adhesion between the printing and PETG filaments that is compromised by printability under lower temperatures. Infrared measurements show that the heat accumulation of PETG during thermal cycling is only captured by a peak temperature of up to 160 °C at a printing temperature of 255 °C. Due to the presence of process-induced porosity, printed specimens within the printing temperature range (240–250 °C) show a low overall density. Based on the density measurement, the amount of porosity varies between 16% and 19%. The results of X-ray micro-tomography contrast with the density measurements as the processing of 3D images indicates a bulk porosity content of only 2% for a 250 °C printing temperature. Table 1. presents some mechanical and electrical characteristics of PETG filament [16].

Table 1

**Mechanical and electrical characteristics of PETG filament [20]**

Mechanical and electrical characteristics	PETG	
	Value	Unit
Density at 20 °C	1.3	g/m <sup>3</sup>
Elastic modulus at 20 °C	2.04	GPa
Elongation at 20 °C	29	%
Flexural strength	68.3	MPa
Melting point	180 - 200	°C
Vicat softening temperature	78	°C

#### 4. RESULTS AND DISCUSSION

This part of the work presents the overview of the calculation of total free-fall time for probe to reach Earth if released in the atmosphere from the height of 21 km. As the properties of the atmosphere vary with height (temperature falls from 288 K to 216 K, density from 1.285 to 0.096 kgm-3 and pressure from 1.01325 to

0.05979 bar, see Fig. 2 and 3) the problem is non-stationary and it would be computationally very demanding. In order to simplify it, we discretize continuous variation of atmospheric properties with height with piecewise constant one for every 500 meters and simulated free fall of the probe in such atmosphere.

The calculation started with a simulation of flow around the axisymmetric body falling with different constant velocities. The resultant calculated force in the vertical direction should be equal to probe weight. We set up different probe weights by simulation of the free-fall velocity at a given height. Then, the calculation of the time needed for the probe to fall 500 m by this constant velocity was performed. Repeating this procedure for all 500 m steps and adding times we calculated the total free fall time of the probe of different masses. The adopted atmosphere air properties (density, pressure) at different heights are given in Fig. 2.

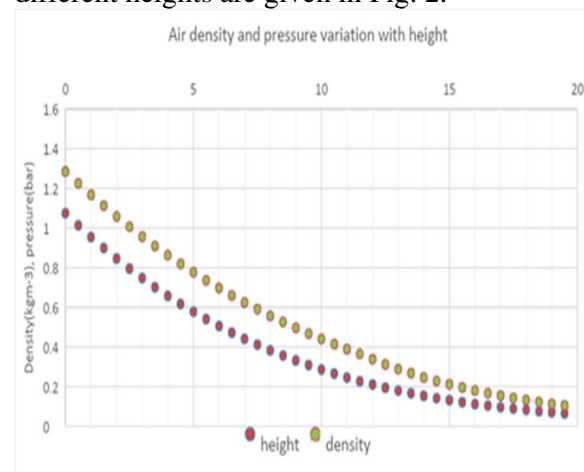


**Fig. 2.** Atmospheric air density and pressure variation with height (A Sample Atmosphere Table)

The resultant velocity field for one simulation with a fall velocity of 10 ms<sup>-1</sup> is shown in Fig.3, rotated anticlockwise by 90 degrees. Fig. 3 shows four different flow zones (in the moving coordinate system fixed to the probe): high pressure/low-velocity zone at the round apex of the probe; high velocity (shown in red)/low pressure at the widest part of the probe; toroidal dead zone of reversed flow at the constriction of the probe and reverse flow zone at the blunt part. The maximum velocity is 2.5 times the inflow velocity (the probe free-fall velocity).

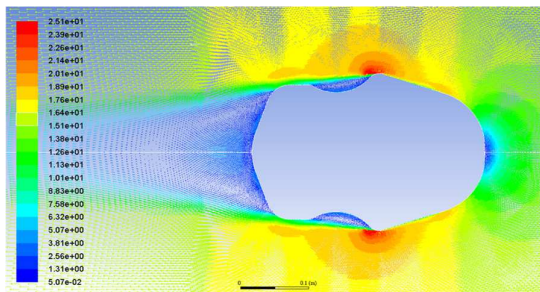


**Fig. 3.** The resultant velocity field with fall velocity of 10 ms-1 (vectors are coloured by speed)

For a set of five different heights (0, 5000, 11000, 19000 and 19500 m) with adequate air densities, pressures, and different velocities we calculated drag force by flow simulation. The resultant values are drawn in Fig. 4 with interpolated polynomials formula. These polynomials were used to calculate free-fall speed for different probes weights.

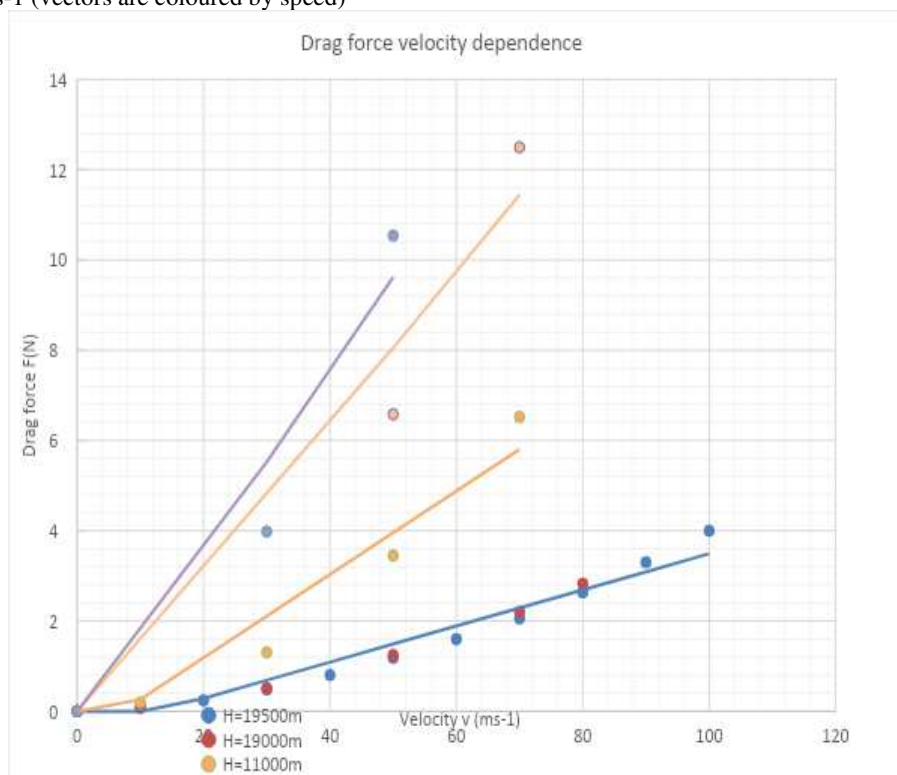


**Fig. 4.** Probe free fall drag force-velocity dependence

For the following three probe masses: 0.2, 0.4, and 0.5 kg the free-fall velocity curves versus height are given in Fig. 5.

Finally, we can calculate total free-fall time for probes of different weights and interpolate the curve (see Fig. 6.).

We find the total free-fall time varies between 602 s and 376 s for probe masses of 0.2 to 0.5 kg.

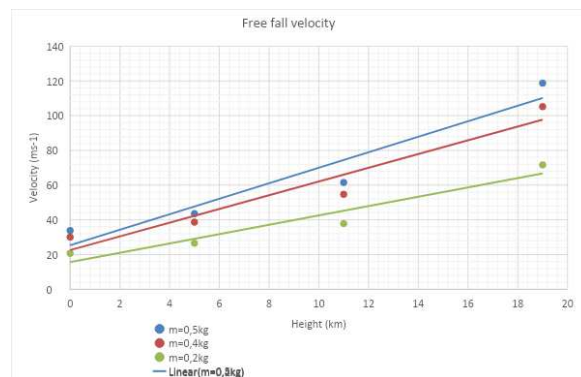


**Fig. 5.** Free-fall velocities at different heights for different probe weights



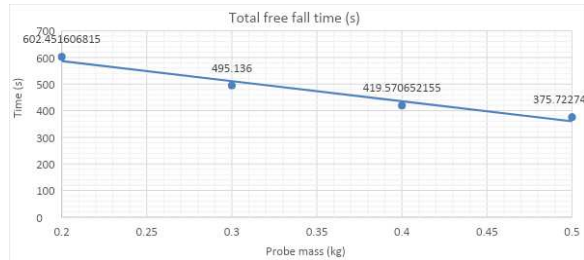


**Fig. 6.** The total probe free-fall time for different probe mass

## 5. CONCLUSIONS

Environmental issues include the loss of natural resources. Many possible solutions have been offered and tried. This paper describes the design and analysis of a very detailed 3D printed prototype. Different instruments for weather and atmospheric measuring can be attached to this 3D probe. The computer simulation of the probe flow through the atmosphere was carried out with Ansys Fluent software. There has been an outpouring of environmentally sustainable filaments that can now be used in 3D printing while maintaining the necessary model characteristics. The proposed performance of this project can potentially predict the environmental effects of a pandemic situation. The design of the 3D model was explained in detail through all phases of computer modelling, including the first, CAD phase, and the second, CAD/CAM phase. Different stages are shown with structural cross-sectional details. The theoretical argument behind the computer simulation is measured by the average free-fall time that is provided by a 21 km drop and the trip through the atmosphere. The resultant velocity field with chosen fall velocity was simulated. We have calculated the drag force of the presented model from our experiments and computations by modelling the flow of a fluid that goes through atmospheric air in various vertical positions. This simulation experiment provides the free-fall velocity curves versus height for three sample masses: 0.2, 0.4, and 0.5 kg.

Finally, we quantified the total probe free free-fall time for different probe mass. The lack of existing suitable institutional instruments of biodegradable 3D printed filaments is one

reason why the probe is not yet printed and put into use. Our next paper's topic will include 3D printing of this probe with professional manufacturing equipment.

## ACKNOWLEDGMENT

This article was made under the support of the projects “3D and Virtual Reality Technologies for VET”, 2019-1-HR01-KA202-061006. And “Boosting the scientific excellence and innovation capacity of 3D printing methods in pandemic period – BRIGHT”, 2020-1-RO01-KA226-HE-095517. The authors would like to thank prof. Lado Kranjcevic from the University of Rijeka, Faculty of Engineering for the model Ansys Fluent analyse.

## 8. REFERENCES

- [1]European Commission. *European plastics strategy by 2030*. Retrieved May 2, 2022, from [https://ec.europa.eu/commission/press-corner/detail/sv/MEMO\\_18\\_6](https://ec.europa.eu/commission/press-corner/detail/sv/MEMO_18_6)
- [2]Arefin, A.M.E.; Khatri, N.R.; Kulkarni, N.; Egan, P.F. *Polymer 3D Printing Review: Materials, Process, and Design Strategies for Medical Applications*. *Polymers* 2021, 13, <https://doi.org/10.3390/polym13091499>
- [3]Caminero M.A., Chacón, J.M., García-Plaza, E., Núñez, P.J., Reverte, J.M. and Becar, J.P., 2019, *Additive Manufacturing of PLA-Based Composites Using Fused Filament Fabrication: Effect of Graphene Nanoplatelet Reinforcement on Mechanical Properties, Dimensional Accuracy and Texture*, *Polymers* 2019, 11(5), 799
- [4] Somireddy, M., Singh, C.V., Czekanski, A. *Mechanical behaviour of 3D printed composite parts with short carbon fiber reinforcements. Engineering Failure Analysis*.(2019). 107. <https://doi.org/10.1016/j.engfailanal.2019.104232>.
- [5] Ekoi, J.E., Dickson, A.N., Dowling, D.P. *Investigating the fatigue and mechanical behaviour of 3D printed woven and nonwoven continuous carbon fibre reinforced polymer (CFRP) composites*, *Composites Part B: Engineering* (2021) 212,

- <https://doi.org/10.1016/j.compositesb.2021.108704>.
- [6] Wu, H., Fahy, W.P., Kim, S., Kim, H., Zhao, N., Pilato, L., Kafi, A., Bateman, S., Koo, J.H., *Recent Developments in Polymers/Polymer Nanocomposites for Additive Manufacturing*. Progress in Materials Science. (2020) 111. <https://doi.org/10.1016/j.pmatsci.2020.100638>
- [7] Păcurar, A., Păcurar, R., Erőss, B., Miron-Borzan, C. *Optimal Tool Path Strategies For Decreasing The Manufacturing Time Of One Thermoforming Mold*, Acta Technica Napocensis, Series: Applied Mathematics, Mechanics, and Engineering, (2021) 64, Issue I.
- [8] Păcurar, A., Rău, M., Păcurar, R., Guțiu, E., Bacali, L., Cosma, C., *Research regarding the design and manufacturing of hand orthosis by using Fused Deposition Modeling technology*, MATEC Web of Conferences vol. 299, 01008 (2019), <https://doi.org/10.1051/mateconf/201929901008> MTeM 2019.
- [9] Wichniarek R., Hamrol A., Kuczko W., Górski F., Rogalewicz M., *ABS filament moisture compensation possibilities in the FDM process*, CIRP Journal of Manufacturing Science and Technology - 2021, vol. 35, p. 550-559
- [10] Kuczko W., Hamrol A., Wichniarek R., Górski F., Rogalewicz M., *Mechanical properties and geometric accuracy of angle-shaped parts manufactured using the FFF method*, Bulletin of the Polish Academy of Sciences: Technical Sciences (2021) 69(3), e137387
- [11] Mognol, P., Lopicart, D., Perry N., *Rapid Prototyping: energy and environment in the spotlight*. Rapid Prototyping Journal, Emerald, ISSN: 1355-2546, (2006) 12, pp. 26-34.
- [12] Kuznetsov, V. E., Tavitov, A. G., Urzhumtsev, O. D., Korotkov, A. A., Solodov, S. V., & Solonin, A. N. *Desktop Fabrication of Strong Poly (Lactic Acid) Parts: FFF Process Parameters Tuning*. Materials (2019) 12 (13), <https://doi.org/10.3390/ma12132071>
- [13] Abdulhameed O, Al-Ahmari A, Ameen W, Mian SH. *Additive manufacturing: Challenges, trends, and applications*. Advances in Mechanical Engineering. (2019.) doi:10.1177/1687814018822880
- [14] Liu, Z., Jiang, Q., Yang, Z., Li, T., Zhang HC. *Sustainability of 3D Printing: A Critical Review and Recommendations*. Proceedings of the ASME, International Manufacturing Science and Engineering Conference (2016.)
- [15] Gebler, M., Schoot, U., Anton J.M., Visser, C. *A global sustainability perspective on 3D printing technologies*, Energy Policy, Elsevier (2014) 74, pp. 158-167.
- [16] Kalmykova, Y. Sadagopan, M., Rosado, L., *Circular economy – From review of theories and practices to development of implementation tools*, Resources, Conservation and Recycling, (2018) 135, pp. 190-201.
- [17] Engineering Simulation Software Ansys, official documentation, [www.ansys.com](http://www.ansys.com) (last access: 15.3.2022.)
- [18] Maricic, S., Haber, I. M., Veljovic, I., Palunko, I., *Implementation of Optimum Additive Technologies Design for Unmanned Aerial Vehicle Take-Off Weight Increase*. EUREKA: Physics and Engineering, (2020) 6, pp. 50-60.
- [19] Guessasma, S., Belhabib, S., & Nouri, H. *Printability and Tensile Performance of 3D Printed Polyethylene Terephthalate Glycol Using Fused Deposition Modelling*. Polymers, (2019) 11(7), 1220 .
- [20] Matmatch, official catalogue of materials, <https://matmatch.com/> (last access: 21.3.2022.)

### **Simularea caderii libere a unei piese test astronautice realizată prin printare 3D**

**Rezumat:** Această lucrare prezintă conceptul și studiul unui prototip imprimat 3D al unei componente astronautice. Un instrument pentru măsurarea vremii și a atmosferei poate fi utilizat pentru o componentă prototip proiectate având anumite trăsături și caracteristici specifice de proiectare. Datorită dezvoltării semnificative a metodelor de fabricație tehnologice, materialele ecologice pot fi acum utilizate în diferitele tehnologii de printare 3D, păstrând în același timp caracteristicile necesare și specifice ale modelului proiectat. Modelul propus în cadrul acestui articol își propune să analizeze din punct de vedere teoretic influența unor astfel de materiale asupra mediului, aspect deosebit de important mai ales în timpul pandemiei, cum a fost pandemia COVID-19. Sunt prezentate astfel în cadrul acestui articol etapele de modelare ale unui prototip cu aplicabilitate în domeniul astronomic, fiind oferite detaliile de bază structurale în secțiune transversală ale modelului CAD proiectat. Sunt prezentate apoi în cadrul acestui articol de asemenea calculele și simulările care au fost realizate folosind programul Ansys, program utilizat pentru studiul de cădere liberă a acestui tip de produs. Simularea realizată a avut scopul de a determina timpul mediu de cădere liberă a acestui model pe Pământ de la o înălțime de 21 km în atmosferă. Câmpul vitezei de deplasare a modelului a fost determinat în strânsă corelație cu viteza de cădere selectată pentru modelul testat. În cadrul acestei simulări a fost determinată de asemenea forța de tragere a modelului prin simularea de curgere ce a fost realizată pentru un set de 5 înălțimi de lansare diferite a modelului în cadere liberă (0, 500, 11000, 19000 și 19500 m) ținând cont cu precădere de densitatea, presiunea și viteza corespunzătoare a aerului. Curbele de viteză ale modelului aflat în cadere liberă în funcție de înălțimea de lansare a modelului au fost determinate pentru trei tipuri de modele prototip având greutatea diferite: 0,2, 0,4 și 0,5 kg. În cele din urmă, timpul mediu de cădere liberă ale modelelor analizate având diferite greutăți au fost determinate prin interpolarea curbelor generate în cadrul simulărilor realizate cu ajutorul programului Ansys.

**Sven MARICIC**, Associated Professor, Head of Centre for biomodelling and innovations in medicine, Faculty of Medicine University of Rijeka & Juraj Dobrila University of Pula, Croatia, 0038598675204, smaricic@unipu.hr, Ulica Br. Branchetta 20, 51000 Rijeka

**Iva MRSA**, Lecturer, Institute for Science and Technology VISIO, Juraj Dobrila University of Pula, 52100 Pula, 0038598470976, ivamrsahaber@gmail.com, Croatia

**Răzvan PĂCURAR**, Associated Professor, Department of Manufacturing Engineering, Faculty of Industrial Engineering, Robotics and Production Management, Technical University of Cluj-Napoca, B-dul Muncii 103-105, razvan.pacurar@tcm.utcluj.ro, 400641 Cluj-Napoca, Romania

**Zoran MRSA**, Lecturer, Institute for Science and Technology VISIO, Juraj Dobrila University of Pula, 52100 Pula, 0038598403515, zoran.mrsa@gmail.com, Croatia